Optical MEMS enable next generation solutions for robot vision and human-robot interaction

Daniel Lovell, Veljko Milanovic, Abhishek Kasturi, Frank Hu, Karan Soni, et al.

SPIE.

Optical MEMS Enable Next Generation Solutions for Robot Vision and Human-Robot Interaction

Daniel Lovell, Veljko Milanovic, Abhishek Kasturi, Frank Hu, Karan Soni, Derek Ho,

Bryan H. Atwood, Lj Ristic

Mirrorcle Technologies, Inc., Richmond, CA

Xiaomeng Liu, Sanjeev Koppal

University of Florida

ABSTRACT

Robots and drones are presently in the industry's focus to serve a critical role in Industry 4.0 and the Transportation Revolution. Integration of robots and drones in these areas improves efficiency and safety, adds flexibility in operation, and reduces operating costs. However, they are still far from achieving the optimal performance needed to execute autonomous tasks at high levels. As these platforms are battery operated, all sub-systems that augment their capabilities must be low-power solutions. In the case of airborne drones, it is also critical that solutions are ultra-light weight and of small form factor. Additionally, robots will be employed in the modern working environment in tandem with humans, but adequate human-robot interaction and intention communication solutions do not currently exist.

Consequently, MEMS mirrors-based sensing and interaction systems designed for robots and drones are essential as they offer solutions with the lowest power consumption, weight, and cost in high volume. However, existing MEMS Mirror-based solutions have not achieved the necessary compactness and efficiency for robotics.

In this paper we describe and demonstrate MEMS Mirror-based 3D perception sensing (SyMPL 3D Lidar) and animated visual messaging (Vector Graphics Laser Projection with Playzer) systems optimized for robots and drones. These sub-systems each consume <1W in power, at least 10x lower than other solutions in the market, weigh <50g, and have small form factors. Furthermore, we will show that combining these two systems leads to new capabilities and functionalities that meet the demands of robot vision and human-robot interaction.

1. INTRODUCTION

1.1. INDUSTRY 4.0 AND THE TRANSPORTATION REVOLUTION

Robots and drones are presently in the industry's focus to serve a critical role in Industry 4.0 and the Transportation Revolution. Integration of robots and drones in these areas improves efficiency and safety, adds flexibility in operation, and reduces operating costs. Furthermore, massive deployment of autonomous mobile robots (AMRs), automated guided vehicles (AGVs), and drones brings many advantages including space optimization, process optimization, speed, efficiency improvement, and flexibility in handling changes in operations in warehouse management, service, and delivery. However, the deployment of these "smart" machines creates a new working dynamic where interaction between humans and robots is frequently required or inherent by their proximity in the use of the same working area. An obvious example is the increased adoption of service robots in restaurants where they share, operate, and interact with workers and customers. However, these robotics systems are still far from achieving the optimal performance needed to execute autonomous tasks at high levels. In part, this is due to limitations of the 3D perception sensing solutions available today as well as challenges in overcoming the computational complexity of such systems. Even if fully autonomous execution was achieved, there remains a drastic need for better robot-human intention communication solutions to improve the safety and confidence of the humans in their workspace.
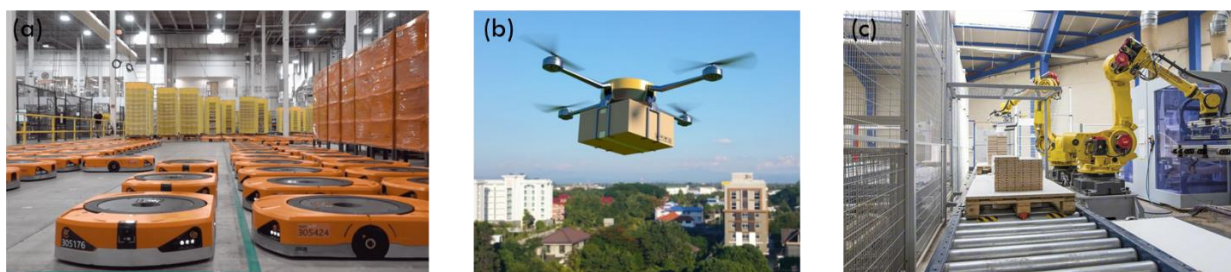

Figure 1. (a) Amazon Robotics "Pegasus" used to transport inventory pallets and pods throughout the warehouse.[1] (b) Concept render of a drone used for last-mile delivery. [2] (c) A pick-and-place robot sorting and stacking wooden panels for assembly. [3]

Toward achieving this safer and more efficient future supported by robots and drones, a variety of new technologies are being developed and adopted. However, in addition to the challenge of meeting critical performance requirements, there is another major restriction in the adoption of new technologies in this market. Namely, since mobile robotics and airborne drones are battery-powered, all sub-systems that augment their capabilities must be very light, compact, and low-power consumption solutions. Especially in the case of airborne drones, these latter features are typically prioritized over some performance parameters.

In this work, we propose that optical MEMS, particularly electrostatic gimbal-less MEMS Mirrors, uniquely enable solutions that offer both high-performance robot vision and human-robot interaction, while at the same time meeting and exceeding the expectations of low weight, compactness, and low power consumption.

1.2. ROBOT VISION SOLUTIONS

Many of the machine vision solutions employed on robotics today are principally camera-based. For some applications, camera-based solutions are acceptable, but for others, a two-dimensional image presents many limitations in deriving critical depth or velocity information. Employing a camera for robot vision frequently requires more processing power and greater pools of memory to process images at sufficient speeds. In some systems, this major computational cost necessitates the inclusion of dedicated hardware acceleration platforms such as GPUs, FPGAs, and ASICs [24]. Naturally, this hardware significantly complicates power and space requirements for mobile robotics and drones. In an effort to address the need for depth information, some camera solutions utilize two stereoscopically arranged cameras to capture depth information (stereo-camera or 3D camera). However, stereo image processing is considered to be one of the most

computationally expensive tasks in computer vision, and the demand for power and space only increases [25]. Furthermore, the heat generated by such a system can overwhelm a drone unless it is in constant motion, and the significant latency required to obtain the 3D data presents major timing limitations. As an alternative approach to accomplish 3D perception sensing with fast rates and low latency, the robot vision market is increasingly looking at lidar.
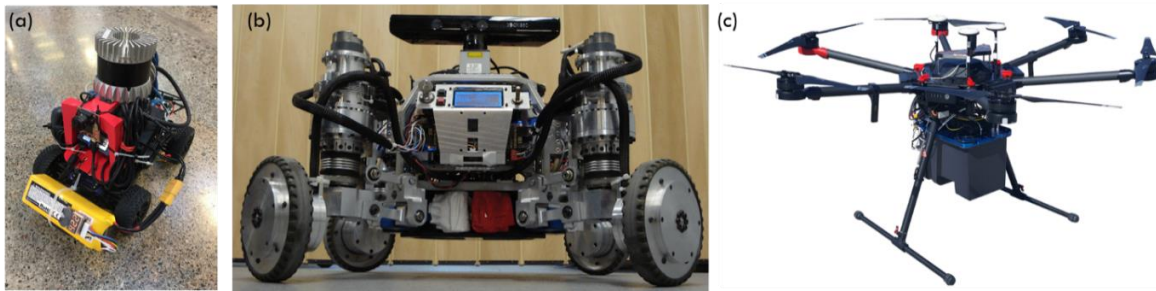

Figure 2. (a) Ouster OS-1-64 sensor mounted on a robot system to perform odometry estimation [13] (b) A Kinect sensor mounted together with a URG-04LX laser rangefinder on the AZIMUT-3 robot platform. The former employs a stereoscopic arrangement to measure depth information [27] (c) A high-payload drone for surveying, equipped with the Teledyne CL-90 4.1 kg LiDAR Scanner [28].

Since cameras are already prevalent in many existing autonomous systems, augmenting the camera's data with additional dedicated sensors such as lidar can help reduce the computational load for the system. Single-point lidars (laser rangefinders) and ultrasonic sensors have been the provisional go-to solutions used in proximity sensing and collision avoidance as the robots and drones are navigating. This is due in part to their availability in the market with competitive small sizes and power consumption. Additionally, lidars are self-illuminated and can operate well in dimly lit areas, at night, or in fully automated warehouses where lighting has been obsolesced. But increasingly complex robot and drone applications demand much more than minimal forward-looking collision avoidance and look to scanned lidars to obtain high resolution, accurate depth information over a large field of view. This provides the robot with significantly more information to help navigate safely and efficiently, detect, classify, sort, and pick objects, and accomplish increasingly autonomous tasks in the presence of other robots and humans. Because of this demand, mechanical spinning 2D and 3D lidars have seen limited adoption in autonomous robotics and drones. However, they are large, heavy, and require tens of Watts to operate, making them a temporary solution mainly restricted to the development of new applications. A small, lightweight, and low power consuming lidar solution is needed to address the needs of the AGV, AMR, and drone markets to offer an efficient long-term solution.

1.3. HUMAN-ROBOT INTERACTION AND INTENTION COMMUNICATION

As robots continue to see expanded use in industrial environments such as warehouses and assembly lines, they are also breaking through into commercial storefronts and restaurants as well as public streets and sidewalks. Robots and drones navigating and operating near humans is often a requirement, and consequently, there exists a strong demand for clear and effective means for human-robot interaction and intention communication. In a 2016 review of the current status of human-robot interaction, Sheridan cites display and supervisory monitoring of automatic action as two of the greatest human factors research needs [20]. Some of the mechanisms presently used for robot intention communication are LCD displays mounted on the robot and auditory cues from embedded speakers. However, displays integrated within the robot present significant visibility challenges for humans beyond close proximity or in outdoor settings. And conditions in industrial facilities and warehouses are notoriously loud and noisy, which significantly hinders sound-based interactions between humans and robots/drones.

This indicates a need for efficient and clear visual messaging that can unambiguously indicate robot intent. The industry has evaluated several methods of communicating robot intent via projection displays from the robot or drone, including projection of present trajectories, current operating status, and planned actions [4][19]. Much of the industry's previous exploration of robot intention communication in the workplace has been centered upon video projector solutions [17][18][22]. However, most warehouse and factory environments also employ especially bright lighting which precludes

existing technologies such as LED or laser-based video projectors for use in these conditions. In this paper, we propose and demonstrate alternative projection solutions that are better suited for these industrial environments.

In their exploration of laser projection systems to address these issues, Wengefeld, et. al evaluated the use of a galvanometer-based laser projector and compare it against LED video projectors. They found that even lower-power LED video projectors consume up to 33W, or 15% of their tested robot's total power profile while not providing desired projection angle and brightness [5]. Indeed, our own previous side-by-side comparisons of DLP projectors, pico-projectors, and Vector Graphics Laser Projection (VGLP) projectors showed significantly greater visible contrast was achieved by the VGLP projectors when compared with DLP projectors or pico-projectors, despite the significantly higher power consumption of the latter two [6]. Furthermore, we demonstrated that when employing electrostatic MEMS Mirror-based VGLP projectors, this high-visibility and high-contrast projection was achieved while only consuming <1.5W total power [6].
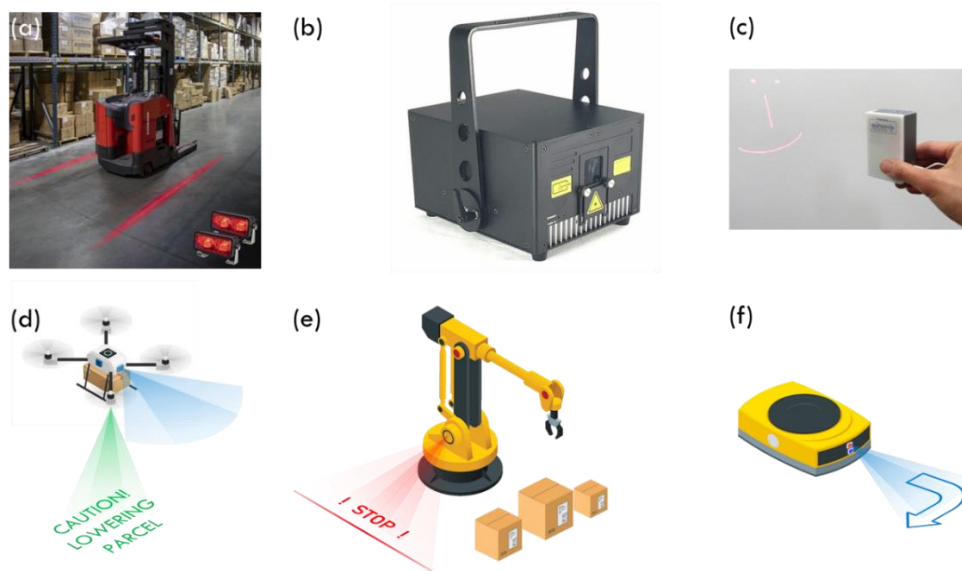

Figure 3. (a) Example of existing human-robot visual messaging on a forklift with LED-based line projectors, (b) a laser-based galvanometer scanner for high brightness vector graphics projection, requiring 10s of W of power and bulky in size and weight, (c) Mirrorcle's pocket VGLP projector solution, the Playzer, which is compact, low power and projects high brightness and high contrast programmable content, (d)-(f) Next-generation robots and drones demand effective solutions for 3D perception sensing and animated visual messaging. High contrast signage, text, graphics, and safety indications improve efficiency and safety in the modern working environment.

Given that a MEMS Mirror based VGLP projector has the highest wall-plug power to visibility efficiency, we believe that it is an ideal solution for human-robot interaction and intention communication. Its low power consumption and small size enable it to be mounted on power-constrained and battery-powered robotics platforms, while its highly contrasted and bright projections are desired for safety and information messaging in loud and bright warehouse settings.

2. MEMS MIRROR SOLUTIONS FOR ROBOTICS SYSTEMS

2.1. GIMBAL-LESS DUAL AXIS MEMS MIRRORS

MEMS mirrors are increasingly recognized as optimal solutions for light steering applications due to their high reliability, decade-plus lifetimes, small form factor, and low power consumption. Presently they are widely used in a range of applications such as biomedical imaging and microscopy, spectroscopy, free-space optical communication, 3D sensing and imaging, lidar, pocket-sized projectors, and projection and heads-up displays [14]. MEMS mirrors are frequently used as replacements for galvanometer scanners and other scanning methodologies where low size, weight, reliability, and low power consumption requirements are prioritized. While there are multiple MEMS mirror technologies and designs in

competition today, it is the electrostatic, single-crystal-silicon based MEMS mirrors that offer the widest operating temperature range [6], highest reliability, and lowest power consumption. This makes them particularly well-suited for integration into space and power-constrained robotics and drone systems.

There are a few distinct variations in the MEMS mirror designs, including single and dual axis steering. They can operate in quasistatic (point-to-point) or resonant only mode. Mirrorcle has an extensive offering of MEMS mirrors from 1.0mm to 7.5mm in diameter with various actuator designs and mirror coatings in Aluminum and Gold [7]. The table below in Figure 4 shows some of the MEMS mirror products, their specifications, and their respective applications.

MEMS Mirror	A7M10.2-1000AL	A7M20.2-2000AL	A8L2.2-4600AL	A8L2.2-5000AU	A5L2.2-6400AU
Package and Cover	TINY48.4-NW	TINY48.4-NW	TINY48.4-A/F/2TP	TINY48.4-NW	TINY48.4-B/W/TP
Mirror Diameter	1.0mm	2.0mm	4.6mm	5.0mm	6.4mm
Optical Angle	±10°	±10°	±10°	±10°	±2.3°
First Resonance	4690Hz	1395Hz	350Hz	300Hz	750Hz
Figure of Merit	highest bandwidth	most versatile	large Theta*Diameter	largest Theta*Diameter	large mirror diameter
Applications	Vector Graphics Laser Projection, 3D sensing	Lidar, 3D sensing and Imaging, FSOC	Lidar, Biomedical Imaging	Lidar, Biomedical Imaging	Free Space Optical Communication (FSOC)

Figure 4. A table of five dual-axis quasi-static MEMS mirror designs used in a variety of beam steering applications, arranged from smallest to largest in diameter, and list of their key characteristics.

2.2. SCAN MODULES – OPTOMECHANICAL INTEGRATION OF MEMS MIRRORS

MEMS mirrors are typically used in beam steering applications which require an optomechanical assembly of the MEMS mirror, with a light source or laser, collimation and beam shaping optics, and projection optics to determine the final output scan's field of view. Beginning in 2010, Mirrorcle has developed an optomechanical solution called the Scan Module, with the latest iteration, EaZy4.0 Scan Module [8][9]. The EaZy4.0 Scan Module is based on the A7M10.2-1000AL MEMS mirror (Figure 4), using off-the-shelf optical and laser components and a custom aluminum chassis, made for projection development and for volume production to be used in any applications. The Scan Module is designed to steer a monochrome laser, violet (405nm), blue (450nm), green (520nm), or red (635nm), over a 34° x 34° field of view, maintaining a beam divergence of less than 2.5mrad, with a repeatability of less than 5 millidegrees. The A7M10.2-1000AL MEMS mirror has a bandwidth of ~2.2kHz when used with simple LPF-based driving [15], allowing it to project text, logos, or any arbitrarily programmable content in vector graphics format at refresh rates up to 60Hz. The Scan Module design is flexible, allowing for a simple change in optics to increase the FOV to address any larger or smaller angles [12] – in such arrangements, the FOV has a fairly simple trade-off with beam divergence. Figure 5c shows an example modification to the Scan Module design, where an additional meniscus lens is used to extend the FOV to >120° on the X-axis.
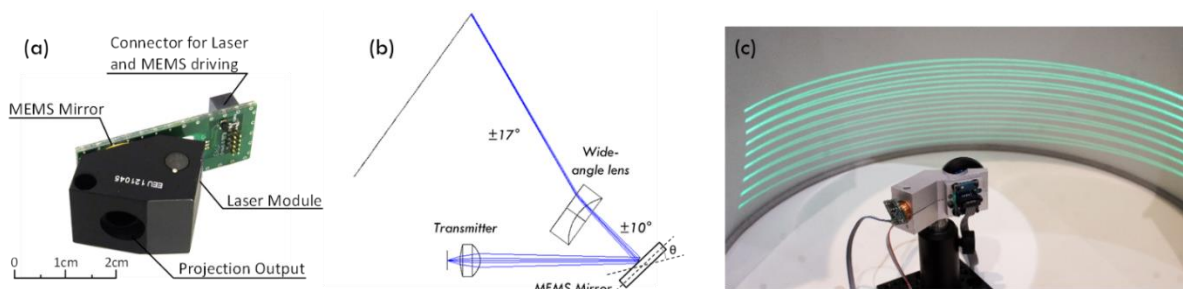

Figure 5. (a) The EaZy4.0 Monochrome Scan Module, (b) the Scan Module's optical train for the EaZy4.0 Monochrome Scan Module, and (c) ultra-wide angle Scan Module with >120° field of regard [12]

Mirrorcle also has a full-color RGB laser Scan Module available for development of new applications. The design is still in early production stages, but it can fundamentally demonstrate the capability of a single MEMS mirror scanning two or more collimated and combined lasers into a single beam, projecting over a 32° x 32° field of view. This RGB laser Scan Module also maintains a beam divergence of less than 2.5 milliradians and positional repeatability of <10 millidegrees.

2.3. CONTROLLER AND DRIVER HARDWARE

Mirrorcle MEMS mirrors are a gimbal-less design, with bi-directional electrostatic rotators that have a unique Biased Differential Quad (BDQ) channel driving scheme, and are driven using compact and low-power consuming high voltage MEMS drivers [10]. There are various options for driving the MEMS devices, starting from a basic driver with analog voltage or digital SPI signal inputs, to higher-level integrated solutions with microcontrollers and FPGAs. The MEMS drivers (Figure 6b) are designed to be compact low power solutions that can be integrated into most end-user electronic designs and consume less than 100mW of power. The onboard boost converter generates the voltage necessary to drive the electrostatic MEMS Mirrors efficiently from the 5VDC supply at the input. Additionally, waveform smoothing hardware low-pass filters are integrated within the driver's four driving channels.
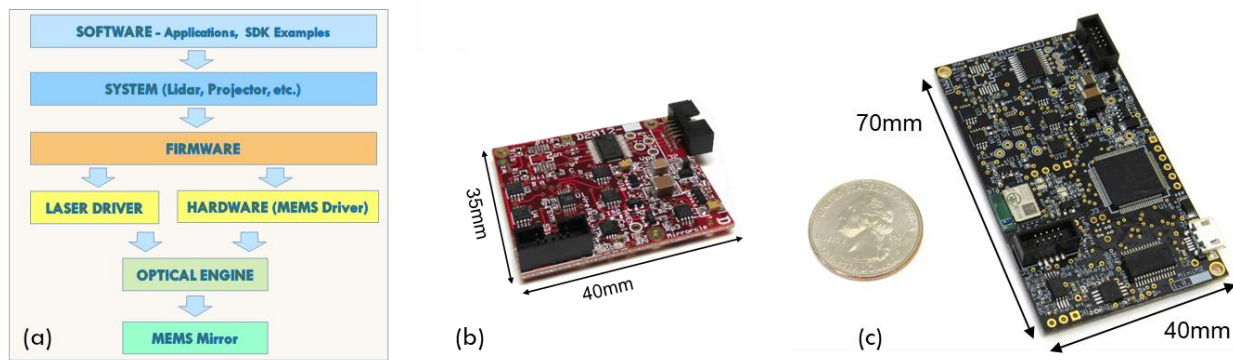

Figure 6. (a) Mirrorcle's comprehensive technical stack for MEMS Mirror-based system solutions; it spans from system-level hardware, firmware, and software down to the MEMS Mirror and Scan Module, (b) a standard Mirrorcle MEMS Driver that receives digital SPI input to drive the MEMS mirror, (c) the MiniMZ MEMS Controller

Mirrorcle currently has a MEMS controller platform based on Microchip's PIC32MZ MCU for development and demonstration purposes, as well as for the platform solutions. The compact OEM version is the MiniMZ controller, which is used in both the SyMPL 3D Lidar and the Playzer. The MiniMZ controller (Figure 6c) is a small form factor controller, 40x70x11mm in size, that is USB powered, and able to communicate via USB COM port, UART, wirelessly via Bluetooth, and provisions available for alternate communication protocols such as Ethernet or CAN bus. The controller has an integrated MEMS driver and monochrome laser driver, and it can mate with a daughterboard that allows it to drive multiple laser channels for RGB applications as well. The controller consumes less than 750mW for communication, API functionality, and to drive the MEMS mirror. For use in robotics applications, several areas of improvement have been identified to reduce this power consumption below 0.5W with standard off-the-shelf electronics and even lower with ASICs.

2.4. SOFTWARE

The MEMS Controller's firmware communicates with the Mirrorcle application programming interface (API). This API abstracts low-level communication with the MEMS Controller and exposes various methods to control the MEMS Mirrors, allowing for the development of more complex control software. To accommodate a wider range of industries, the Mirrorcle API supports multiple platforms and programming languages, with software development kits for Windows, Ubuntu Linux, and Android. On these platforms, we have created libraries for developers to work with the MEMS Controllers using C++, MATLAB, LabVIEW, Java, and Python.

In addition to providing communication and control to the MEMS Controllers, the Mirrorcle API and software development kits are extended to provide scan content generation, scan optimization, interpolation, and filtering functions. These functions are specifically developed for use with Mirrorcle's MEMS Mirrors and MEMS Mirror-based system solutions such as Playzer and the SyMPL 3D Lidar. Users may choose from a variety of scan content generation methods, from parametrized linear raster scans for imaging applications to text and symbol vector graphics for projection applications. Content may then be optimized, interpolated, and filtered using algorithms specifically developed to optimally utilize bandwidth and angle of Mirrorcle's MEMS Mirrors.

3. MEMS MIRROR-BASED SYSTEM SOLUTIONS FOR ROBOTICS

3.1. ANIMATED VISUAL MESSAGING

The smallest and fastest of the dual-axis MEMS mirrors presented above is used as the enabling beam-steering component in Mirrorcle's Vector Graphics Laser Projection (VGLP) Architecture. VGLP combines a full technology stack of software, electronics, and optical laser beam-steering to enable fully programmable and re-configurable laser projection and display of bright, high-contrast graphic content on a variety of surfaces. Mirrorcle has been developing the VGLP system since 2005, presenting prior work for Head-Up Displays, laser-based tracking and imaging solutions, and programmable lighting solutions [6]. Over the years, there have been improvements in the MEMS mirror designs to increase device bandwidth, controller designs to reduce size, weight, and power consumption, and the development of firmware and API layers for easy-to-use applications in various platforms such as Windows, Linux, and Android.
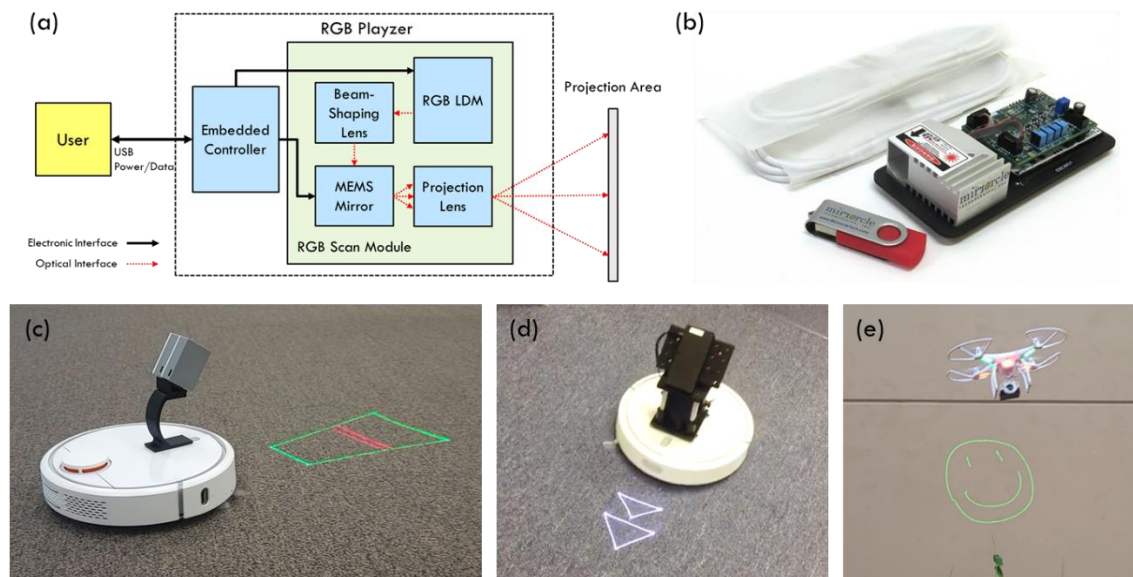

Figure 7. (a) Diagram depicting the RGB Playzer's architecture, including electronic and optical interfaces. Users interact with the RGB Playzer over USB. (b) The OEM version of the RGB Playzer Development Kit (PZDK-03RGB). (c) Two boxed and battery-powered Monochrome Playzers are mounted onto a Xiaomi Mi Robot Vacuum. They project a high-contrast animated graphic in front of the robot. (d) An RGB Playzer mounted above a Xiaomi Mi Robot Vacuum; it projects bright white animated arrows indicating the direction of movement. (e) A DJI P330d consumer drone equipped with a battery-powered Monochrome Playzer. The Monochrome Playzer's projection can be modified in-flight over Bluetooth.

The current solution, Playzer, is a pocket-sized programmable vector graphic laser projector that consists of a MEMS Mirror-based Scan Module and an embedded Controller. It is a compact and low-power solution for displaying graphics in a multitude of environments, both outdoor and indoor. The Monochrome Playzer used in application prototyping is

packaged into a handheld box, 30 x 55 x 80 mm in dimensions, weighing under 70g, consuming approximately 1.5W of power with a fully powered green laser output. The RGB Playzer is an open box (OEM) solution currently still in active development, with a similar size and weight to the monochrome Playzer, and with the additional power consumption of the two added laser diodes, totaling around 2.5W with fully powered RGB output. In both Monochrome and RGB cases, the majority of the power is consumed by the single-mode laser diodes, which have relatively low efficiencies ranging from 8%-30%.

Playzer offers a solution through the VGLP architecture, providing high contrast visual messaging for applications in robotics. The Mirrorcle API is implemented as an interactive and dynamic platform and is made as flexible as possible to allow a variety of ways to import signage content from third-party software, scripts, ILDA files, etc. Furthermore, we improve upon the aforementioned Mirrorcle API to develop the Playzer software API and tools to streamline content creation for use on robotics [8].

As shown in Figure 7, the first step in the VGLP projection process is the choice of signage (image, symbol, graphic) that the user chooses to project. Next, this image is converted to a vector graphic in one of many available applications: it can be converted from a bitmap image to an outline vector graphic, or it can be directly created in one of our software applications as a full-color vector graphic. To fully define such a vector graphic, we must define all of the vector "keypoints" (X-coordinates, Y-coordinates, and color of the segment to follow) as well as time parameters such as the refresh rate (frame rate) in Hz, and sample rate (actual DAC samples for Controller output). This fully defined keypoint construct is termed a "glyph" and can be efficiently stored in the Controller's RAM or Flash memory. This waveform (list of samples) passes through linear transforms that allow for adjustment of any scale, offset, and rotation about any axis. Additionally, transforms for projection angle (perspective) can be applied which allow the projector to be aimed at almost any angle with respect to the target surface. This is especially useful in cases such as projecting a trajectory indicator from the robot down onto the floor ahead of it. In some cases, the sample waveform also undergoes nonlinear transforms that correct nonlinearities added by wide-angle optics or other system imperfections [15]. The flexibility of the vector graphics laser projection architecture allows for all types of transforms and corrections (e.g., lookup tables) to be performed on the data as the hardware system fundamentally allows for control of laser beam position and velocity/time, and therefore is fully flexible to be programmed arbitrarily in any region of the field of regard.
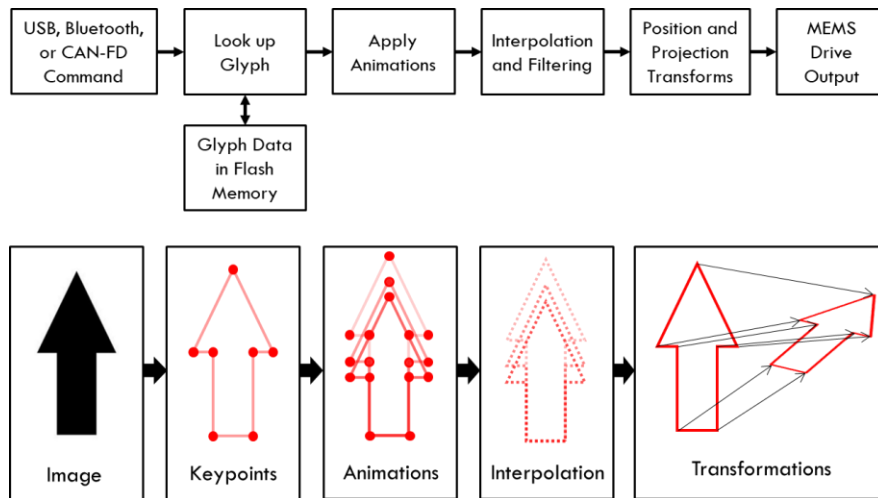

Figure 8. (Top) VGLP software flow, beginning with a USB, Bluetooth, or CAN FD command through to the MEMS Driver Output. (Bottom) Example of the software flow used to generate an animated VGLP arrow which may be used by the robot to indicate trajectory or other critical motion information.

To facilitate simple integration of the Playzer projector onto various types of animated visual messaging systems, robotics or otherwise, the Playzer software and API share the same language and platform offerings afforded by employing the Mirrorcle API. This includes C++, MATLAB, Java, and Python for Windows, Linux, and Android operating systems. Further extending the portability of the Playzer system, we developed interfaces at a lower layer of integration including

serial ASCII and binary commands over USB and direct laser beam steering using analog input. This latest development, called PlayzerX, trades the extensive Playzer software API for wider portability across systems at the user's discretion. Robotics platforms that are closer to bare metal, or that are not compatible with existing Playzer software, may find PlayzerX to be the ideal level of integration.

3.2. 3D PERCEPTION SENSING

MEMS mirror-based 3D perception sensing systems typically requires larger diameter MEMS mirror to transmit or receive more photons for the optical sensor. Mirrorcle has larger diameter mirrors such as the A7M20.2-2000AL 2.0mm diameter mirrors and larger A8L2.2-5000AU 5.0mm diameter mirrors currently in-use in a number of industry MEMS Lidar systems. Mirrorcle has also internally developed the SyMPL 3D Lidar system, which was presented in 2020 at Photonics West, in San Francisco, CA [16]. Since the work presented in 2020, Mirrorcle has further developed the SyMPL 3D Lidar into a more compact solution, that is able to scan a larger 45° x 25° FOV with scan repeatability of <5 millidegrees. The scanning is furthermore fully programmable over that FOV with the option of single-point, line, raster, and other measurement modes. The SyMPL 3D Lidar has also been improved to run and communicate via a single USB connection while consuming less than 1.5W of power.
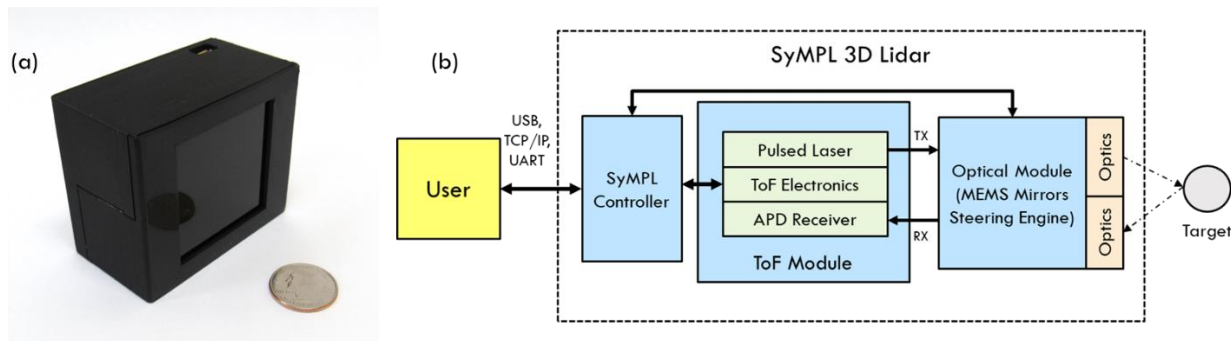

Figure 9. (a) The latest prototype of the SyMPL 3D Lidar, featuring a 45° x 25° FOV, weighing 50g in its OEM version, and consuming ~1W total power. (b) An architectural diagram of the SyMPL 3D Lidar. The user interfaces with SyMPL over USB, TCP/IP, or UART interfaces/protocols. The ToF Module then interfaces with the MEMS Mirrors contained in the Optical Module to scan, range, and generate a point cloud.

The underlying technology of the SyMPL 3D Lidar is still two Mirrorcle MEMS mirrors scanning and receiving the laser light pulses for time-of-flight measurements, and the MTILidar-based API layer enables programmable scanning patterns and streaming of 3D point cloud data over TCP/IP sockets. The Lidar uses the MiniMZ MEMS controller to drive the MEMS mirrors and interfaces with a time-of-flight module to transmit and receive the nanosecond laser light pulses, and calculate the time of flight to determine the distance (Z-axis) to the object. The X and Y axis positions of the 3D point cloud are determined by the MEMS mirror position during the scan, which can be fully programmable to scan the entire field of view or narrow down to specific regions, with adjustable pixel and line densities.
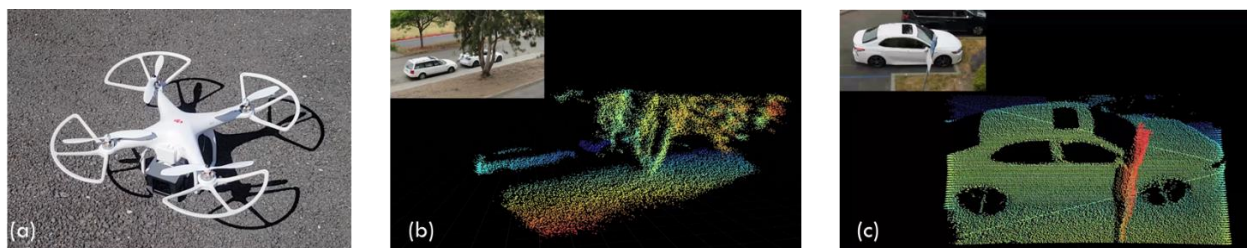

Figure 10. (a) SyMPL 3D Lidar mounted on a drone. (b) Drone mounted SyMPL 3D Lidar scans and generates a point cloud of a tree and two parked cars. (Right) Drone-mounted SyMPL 3D Lidar scans a high-resolution point cloud of a parked car.

We have demonstrated communication with the SyMPL wirelessly using Bluetooth and mounted the system onto a DJI drone to take aerial scans and generate 3D point clouds of objects up to 20m away (Figure 10). The latest SyMPL 3D Lidar (45° x 25° FOV) weighs 50g in its OEM version for integration into a robot or drone platform, with the goal of achieving 25g in the final product. The prototype, in a plastic housing seen in Figure 9a, has approximate dimensions of 75 x 60 x 45mm, consumes ~1W of power, providing a robust low-cost mass-production solution for robotics and drone applications.

4. FUSION OF SOLUTIONS ENABLES NEXT GENERATION APPLICATIONS

In an effort to simultaneously achieve desired sensing and animated visual messaging features on robotics systems, we propose and implement a closely integrated combination of sensor and VGLP projector. Fusing sensors with VGLP projectors at a low-level enables a highly responsive tandem system for sensing and actuation. Using this fused system, we are able to demonstrate low latency animated visual messaging interaction using Playzer based upon data being streamed from the modular sensor. Tight interaction between these two systems increases the reliability and efficacy of safety and informational messaging of robots cooperating with humans in workplaces.

Furthermore, this fusion of solutions allows for decreased overall bill-of-materials costs and enables the development of shared ICs and optical assemblies.

4.1. PLIDAR – 3D PERCEPTION SENSING & ANIMATED VISUAL MESSAGING

We implement a closely integrated combination of the SyMPL 3D Lidar and Playzer – called PLidar. The PLidar system combines our work on the Vector Graphics Laser Project architecture and our 3D Synchronized MEMS Pair Lidar (SyMPL) [6][16]. This combination is achieved by connecting these two systems at a platform layer between the two MCUs and the final top-level software application. To interface this platform layer with the application layer, we unify the VGLP projector and SyMPL 3D Lidar software APIs. As discussed later, this greatly simplifies the development of features and applications that depend on the synchronicity of the two systems.
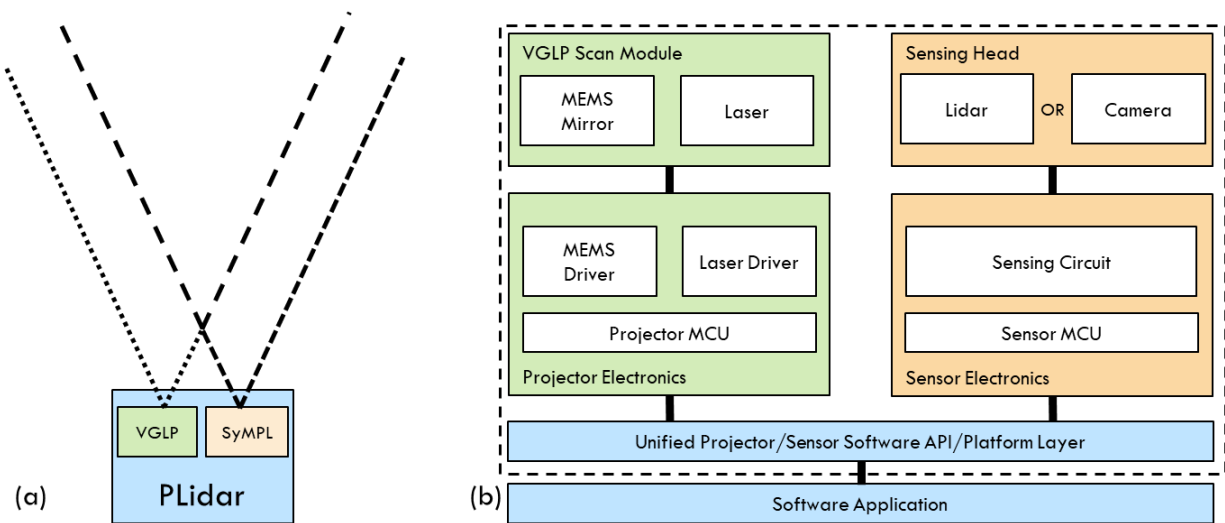

Figure 11. (a) Top-level diagram of PLidar system, combining Playzer VGLP projector with MEMS-mirror based SyMPL 3D Lidar. (b) Lidar in the case of the PLidar system. Camera in the case of the PCamera system. System diagram that depicts the architecture for simultaneous animated visual messaging and perception sensing.

The decision to unify the two systems by integrating them at the electronics layer results in a significant reduction in latency and subsequently allows the development of additional features. With minimal communication overhead, low latency between the lidar and the Playzer can be utilized to create real-time graphics and messaging based on lidar data. Namely, warning and safety symbology can be quickly projected from the robot, based upon, for example, obstacle

proximity. Furthermore, this low latency is critical for real-time informational displays that convey the robot's state and sensor measurements.

To demonstrate PLidar's combined features, we develop a reference implementation using the small and low-power TurtleBot 3 Burger robotics platform from Robotis and Open Source Robotics Foundation. This battery-powered, small form-factor robot includes a Raspberry Pi 3 Single Board Computer (SBC), the OpenCR control module for ROS, two DYNAMIXEL XL430-W250-T motors, and an 11.1V 1800mAh Li-Po battery. We then integrate two monochrome Playzer vector graphics laser projectors and a SyMPL 3D Lidar sensor to enable simultaneous 3D perception sensing and animated visual messaging. This demonstration aims to validate MEMS Mirror-based solutions as providing desired sensing and messaging features while minimizing both power and mechanical design footprints.

We made several modifications to the platform by removing the included 2D lidar and mounting two monochrome Playzer vector graphics laser projectors and a SyMPL 3D Lidar sensor in its place. Additionally, we bypassed the OpenCR control module by using Robotis's U2D2 power hub set, allowing the Raspberry Pi to directly communicate with the DYNAMIXEL motors via UART over USB. This allowed for minimal communication overhead between the motors, Playzers, and SyMPL, and decreased response time from detection of obstacles to issuing motor commands and updating the Playzer projectors. Finally, we included a portable 5V 3000mAh battery which served as the sole power supply for the two monochrome Playzers and SyMPL 3D Lidar. The final hardware architecture is shown in Figure 12a.
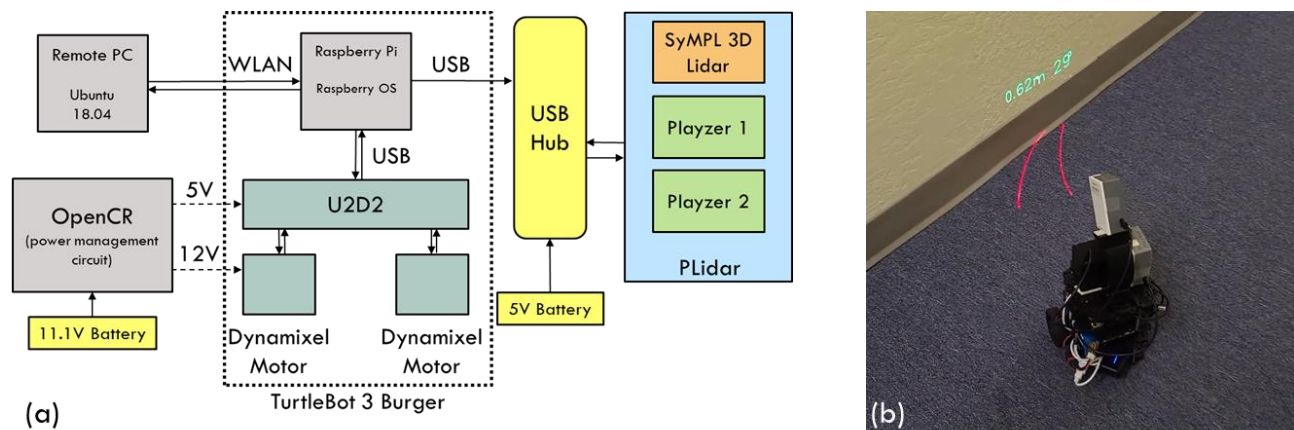

Figure 12. (a) Overview of a PLidar reference implementation on the TurtleBot 3 Burger. (b) PLidar system mounted on the TurtleBot 3 Burger; it measures and displays the distance and angle of the ahead wall in real-time.

The software of the PLidar system is implemented as an extension of the existing Playzer and MTILidar APIs for both the VGLP architecture and SyMPL 3D Lidar. The MEMS Controllers' firmware communicates with an extensive, multi-platform application programming interface (API) that is adapted to support both Playzer and the SyMPL. The software for this demonstration was written to run on the Raspberry Pi SBC which hosted Ubuntu Linux 16.04.

In order to create bright and effective animated visual messaging for intention communication, we utilize the Playzer API to generate arbitrary and programmable vector graphics content. This content, whether it is text, signage, or symbols, can either be calculated and streamed directly to the Playzers at runtime, or it may be pre-processed into glyphs that are stored in the PLidar Controller's flash memory. This latter feature can be particularly useful for robotics platforms with limited memory, or where streaming from off-chip memory can hinder normal operation. In Figure 12b we show the PLidar system integrated with the TurtleBot 3 Burger, where the SyMPL 3D Lidar scans the region ahead of the robot, detects the presence of a wall, and then measures the distance and angle of the wall. These measurements are streamed in real-time to the lower Playzer (green laser) which projects this measurement. Simultaneously, the second Playzer (red laser) incorporated in the PLidar system interfaces with the control software on the TurtleBot to project the present trajectory in real-time, represented as two lines with magnitudes and radius of curvature proportional to speed and direction.
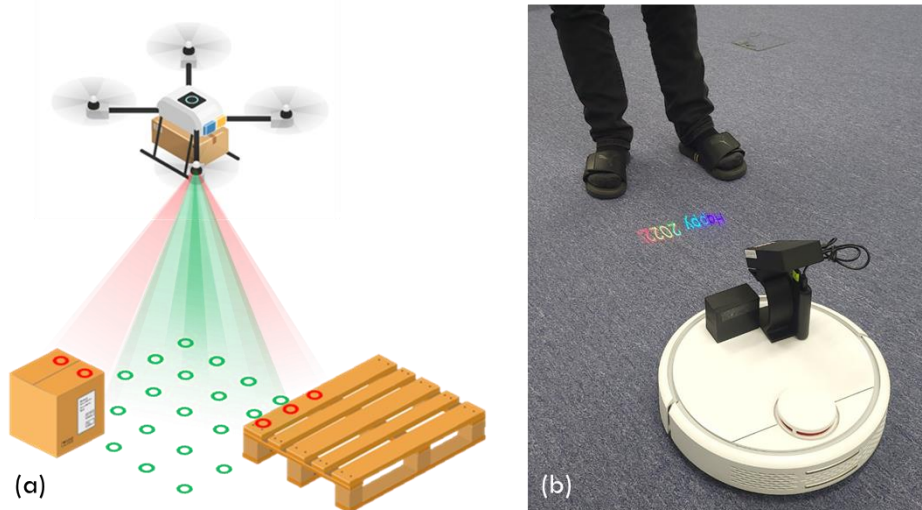
Figure 13. (a) An example application where the PLidar system is used to assist in drone landing. The SyMPL 3D Lidar monitors altitude and detects obstacles in the landing zone. The Playzer is used to project a representation of these measurements and alert nearby workers. (b) PLidar mounted on the Xiaomi Mi robot vacuum cleaner; in this demonstration, it detects the presence of a person and projects "Happy 2022!" using the full-color RGB Playzer.

4.2. PCAMERA – CAMERA & ANIMATED VISUAL MESSAGING

We similarly extend the fused projector-sensor system to demonstrate a side-by-side fusion of a high-speed RGB camera with the Playzer [23]. The goal of this fusion, which we refer to as PCamera, is to enable fully programmable visual messaging and illumination integrated within a camera's field of view. With these two systems closely calibrated, the PCamera uses a pixel-to-angle look-up table to enable the Playzer projector to arbitrarily and accurately address any pixel within their overlapping fields of view. This is accomplished via a side-by-side optomechanical setup that overlaps the camera's field-of-view (FOV) and the MEMS Scan Module's field-of-regard (FOR). With the MEMS Scan Module's FOR fully contained within the camera's FOV, we calibrate a pixel-to-angle lookup table (LUT) that correlates a pixel in the camera's frame to a specific. The camera is thereafter capable of identifying features and objects in its FOV, and employ the Scan Module's point-to-point beam steering features to arbitrarily illuminate and interact with the target. The Playzer and the camera remain connected at the platform layer, with the Playzer's MCU capable of interfacing with the camera's I/O interface. To simplify and facilitate the use of PCamera, we develop an API that further unifies the two systems at the application layer.

It is important to note that the PCamera optomechanical mounting depicted in Figure 12b is nominally bistatic, where the camera FOV and Scan Module FOR do not share exactly the same origin. This can result in some accuracy error due to parallax, specifically at shorter distances (<0.5m). In future designs or revisions of this optomechanical mounting, we consider a coaxial arrangement of the camera and the Scan Module – such as one accomplished via beam splitter by Richter, et. al. [21]. Such an arrangement would eliminate parallax and subsequently increase the accuracy of the pixel-to-angle calibration across wider ranges.

We have further developed the PCamera system into a readily available demonstrator kit, the Laser Scan and Camera Sense Demonstrator Kit (DEMO-02). This demonstrator kit, shown in Figure 13a, implements the EaZy4.0G Scan Module, a complete optomechanical cell housing the MEMS Mirror, green 520nm laser module, and optics. The camera used to complete the PCamera fusion is a USB 3.0 Camera with a 6mm lens for ~45°x 34.5° FOV, a resolution of 720x540 pixels, and up to 500 fps capture rates. The Scan Module and the camera are combined at the USB-SL MZ MEMS Controller, which embeds onboard MEMS and laser driver circuits as well as performs hardware triggering of the camera using its digital synchronization port.
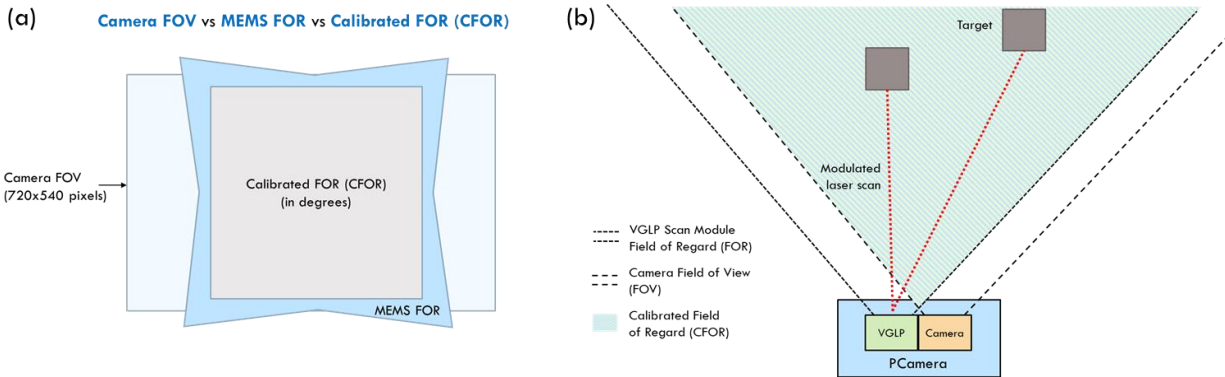
Figure 14. (a) A diagram from the perspective of the PCamera aperture that depicts the overlapping FOV and FOR of the camera and Scan Module. The pincushion-shaped MEMS FOR is a result of projecting the Scan Module's spherical scanning region onto a plane. (b). A top-down diagram of the PCamera's optomechanical mounting that places the VGLP projector and camera to have substantially overlapping FOV and FOR.

Using the Mirrorcle API and the Basler Ace software, we developed a software framework to calibrate, visualize, and utilize the calibrated field-of-regard (CFOR) via a pixel-to-angle inverse look-up table (iLUT). To accurately calibrate the pixel-to-angle lookup table, we first define the calibrated field-of-regard as the angular space within the camera's FOV which is addressable by the Scan Module's FOR. We then calibrate this CFOR with respect to a variably-sized matrix of Scan Module position commands. This results in an inverse lookup table which stores a table of normalized Scan Module positional commands (x, y) corresponding to a uniform table of optical angle locations (θ_x, θ_y).
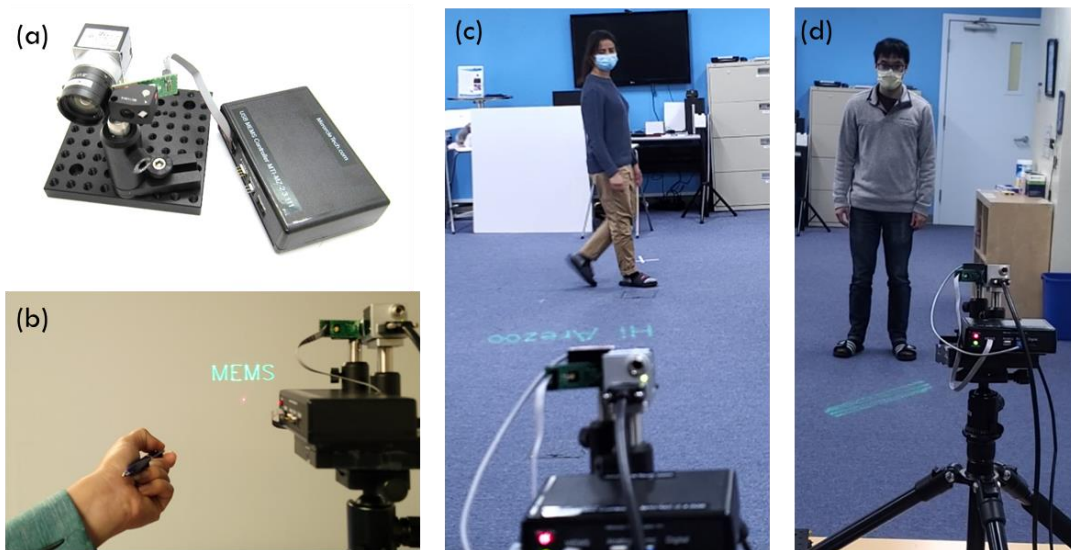

Figure 15. (a) The Laser Scan and Camera Sense Demonstrator Kit (DEMO-02) is used to demonstrate the features of PCamera's combined VGLP and camera system. (b) The PCamera system tracks a laser pointer's spot with projected text from the Scan Module "MEMS". (c) The PCamera system uses computer vision to track a human and project a personalized greeting at their feet or (d) an animated pattern.

This framework was then used to demonstrate several applications of the PCamera system. These demonstrations include a Go-To-Pixel demo which precisely moves the laser to a point clicked by the user in the camera's FOV and a laser pointer tracking demo where the PCamera system tracks a red laser spot with the green text "MEMS" so long as it remains within the CFOR. This latter demonstration is accomplished via filtering and thresholding frames provided by the camera. We

also showcase the ability of the PCamera system to track and illuminate multiple objects, whereby several distinctly contrasting objects within the camera's view are illuminated by the Scan Module with laser spots or letters denoting their relative size.

Finally, and perhaps most relevant to applications on-board autonomous mobile robotics or drones, is a demonstration of PCamera which leverages computer vision to detect humans within the camera's FOV. Using OpenCV, we apply the Histogram of Oriented Gradients (HOG) feature descriptor to the camera's latest capture frame [11]. This provides a bounding box of pixel coordinates where the person is located. We then utilize the PCamera system to project visual messaging content at the base of the bounding box, allowing for information to track the person as they traverse the PCamera's CFOR. This can be used to draw attention to safety messaging, project personalized messages, or otherwise communicate information directly to persons sharing the space with the operating robot. This demonstration is shown below in Figure 15c and Figure 15d.

5. CONCLUSIONS

In this paper we have reviewed the current state of animated visual messaging and 3D perception sensing solutions for use on robots and drones. Furthermore, we have reviewed the effectiveness and suitability of common industry solutions for robot-human intention communication. Although significant progress has been made recently in these areas, the existing solutions frequently struggle to meet feature requirements to be optimal for use in robotics. In the case of robot-human interaction and intention communication, present solutions are particularly lacking in performance and efficiency. In an attempt to address these shortcomings, we propose and describe MEMS Mirror-based systems for 3D perception sensing and animated visual messaging systems optimized for robots and drones. We have demonstrated that the performance of these products is optimized for use in robotics on several levels. First, they are ideal for battery-operated machines such as mobile robotics and drones due to their low power consumption, small form factor, and low weight. Second, Playzer offers especially high contrast animated visual messaging in the presence of bright light which is a typical working condition in production facilities and warehouses. Achieving high-contrast visual messaging in those working conditions is a feature that we believe no other technology presently offers. Third, we have demonstrated further improvements upon these optical MEMS-based systems by fusing VGLP technology with both lidar and a camera to create a new class of products with expanded features and performance named PLidar and PCamera, respectively. Finally, we firmly believe that these fusions of MEMS Mirror-based programmable beam steering solutions with other sensing devices and technologies offer unique capabilities and specifications that will open the gate for further development in robot and drone applications.

6. REFERENCES

[1] Waredock. "What is Amazon Robotic Fulfillment Center?" June 1, 2021. https://www.waredock.com/magazine/what-is-amazon-robotic-fulfillment-center/

[2] PYMNTS. "Are Drones the Future of Last-Mile Delivery for Medicine – and Retail?" May 20, 2019. https://www.pymnts.com/news/retail/2019/zipline-drones-delivery-wings/

[3] Interlake Mecalux. "Pick and place: robots never tire." March 22, 2021. https://www.interlakemecalux.com/blog/pick-and-place

[4] Matsumaru, T., "Mobile Robot with Preliminary-announcement and Display Function of Forthcoming Motion using Projection Equipment," The 15th IEEE International Symposium on Robot and Human Interactive Communication (RO-MAN06), Hatfield, UK, September 6-8, 2006.

[5] Wengefeld, T., Höchemer, D., Lewandowski, B., Köhler, M., Beer, M., Gross, H., "A Laser Projection System for Robot Intention Communication and Human Robot Interaction," 2020 29th IEEE International Conference on Robot and Human Interactive Communication (RO-MAN), Virtual Conference, Aug. 31-Sept. 04, 2020, pp. 259-265.

[6] Kasturi, A., Milanović, V., Hu, F., Kim, H. J., Ho, D., Lovell, D., "MEMS Mirror Module for Programmable Light System" SPIE 2019 OPTO Conference, San Francisco, CA. February 3, 2019

[7] Mirrorcle Technologies. "Mirrorcle Products List." Sep. 2021 https://www.mirrorcletech.com/pdf/Mirrorcle_Products_List.pdf

[8] Mirrorcle Technologies. "Mirrorcle Playzer Integration in Robots and Drones – Q2/2021." Retrieved November 13, 2021. https://mirrorcletech.com/playzer-promotion/

[9] Mirrorcle Technologies. "Mirrorcle Playzer Technology – Product Overview." Retrieved December 23, 2021. https://mirrorcletech.com/pdf/Mirrorcle_Playzer_Technology_-_Overview.pdf

[10] Milanović, V., "Linearized Gimbal-less Two-Axis MEMS Mirrors," 2009 Conference on Optical Fiber Communication, San Diego, CA, USA, Mar. 22-26, 2009, pp. 1-3

[11] Dalal, N., Triggs, B., "Histograms of oriented gradients for human detection," 2005 IEEE Computer Society Conference on Computer Vision and Pattern Recognition (CVPR'05), 2005, pp. 886-893 vol. 1, doi: 10.1109/CVPR.2005.177.

[12] Milanović, V., Castelino, K., McCormick, D., "Highly Adaptable MEMS-based Display with Wide Projection Angle," 2007 IEEE 20th International Conference on Micro Electro Mechanical Systems (MEMS), Hyogo, Japan, Jan. 21-25, 2007, pp. 143-146

[13] Selby, W., "Odometry Estimation with an Ouster OS-1 lidar Sensor," wilselby.com, June 5, 2019

[14] Milanović, V., Kasturi, A., Hachtel, V., "High brightness MEMS mirror based head-up display (HUD) modules with wireless data streaming capability," Proc. SPIE 9375, MOEMS and Miniaturized Systems XIV, 93750A, San Francisco, CA, USA, Feb. 27, 2015

[15] Milanović, V., Kasturi, A., Yang, J., Hu, F., "Iterative Learning Control Algorithm for Greatly Increased Bandwidth and Linearity of MEMS Mirrors in LiDAR and Related Imaging Applications," SPIE 2018 OPTO Conference, San Francisco, CA, Feb. 2018

[16] Kasturi, A., Milanović, V., Lovell, D., Hu, F., Ho, D., Su, Y., Ristic, L., "Comparison of MEMS Mirror Lidar Architectures," SPIE 2020 OPTO Conference, San Francisco, Feb 2020

[17] Vogel, C., Walter C., Elkmann, N., "A Projection-based Sensor System for Safe Physical Human-Robot Collaboration," 2013 IEEE/RSJ International Conference on Intelligent Robots and Systems (IROS), Tokyo, Japan, Nov. 03-07, 2013, pp. 5359-5364

[18] Andersson, N., Argyrou, A., Nägele, F., Ubis, F., Campos, UE., Ortiz de Zarate, M., Wilterdink, R., "AR-Enhanced Human-Robot-Interaction - Methodologies, Algorithms, Tools," 6th CIRP Conference on Assembly Technologies and Systems (CATS), Procedia CIRP, Vol. 44, 2016, pp. 193-198

[19] Vogel, C., Walter C., Elkmann, N., "Exploring the possibilities of supporting robot-assisted work places using a projection-based sensor system," 2012 IEEE International Symposium on Robotic and Sensors Environments Proceedings, Magdeburg, Germany, Nov. 16-18, 2012, pp. 67-72

[20] Sheridan, TB., "HUMAN-ROBOT INTERACTION: STATUS AND CHALLENGES," Human Factors, Vol. 58, no. 4, June 2016, pp. 525-532

[21] Richter, S., Stutz, M., Gratzke, A., Schleitzer, Y., Krampert, G., Hoeller, F., Wolf, U., Riedel, L., and Doering, D., "Position sensing and tracking with quasistatic MEMS mirrors," Proc. SPIE 8616, 86160D (2013); doi: 10.1117/12.2009439

[22] Zaeh, MF., Vogl, W., "Interactive Laser-Projection for Programming Industrial Robots," 2006 IEEE/ACM International Symposium on Mixed and Augmented Reality, Santa Barbara, CA, USA, Oct. 22-25, 2006, pp. 125-128

[23] Mirrorcle Technologies. "Laser Scan and Camera Sense Demonstrator Kit – Overview." Retrieved December 23, 2021. https://mirrorcletech.com/pdf/DEMO/Mirrorcle_DEMO-02_-_Overview.pdf

[24] Feng, X., Jiang, Y., Yang, X., Du M., Li X., "Computer vision algorithms and hardware implementations: A survey," Integration, Vol. 69, Nov. 2019, pp. 309-320.

[25] Michalik, S., Michalik, S., Naghmouchi, J., Berekovic, M., "Real-time smart stereo camera based on FPGA-SoC," 2017 IEEE-RAS 17th International Conference on Humanoid Robotics (Humanoids), 2017, pp. 311-317.

[26] Labbe, M., Michaud, F., "Online global loop closure detection for large-scale multi-session graph-based SLAM," IEEE International Conference on Intelligent Robots and Systems. 2661-2666. 10.1109/IROS.2014.6942926.

[27] Teledyne Geospatial, "Survey-Grade Drone LiDAR Sensors & AI-Based Data Processing Software," https://www.unmannedsystemstechnology.com/company/teledyne-geospatial/, retrieved Dec 28, 2021.